# USING SRTM TO QUANTIFY SIZE PARAMETERS AND SPATIAL DISTRIBUTION OF ENDORHEIC BASINS IN SOUTHERN SOUTH AMERICA

Ralf Hesse
Department of Geography
Friedrich Schiller University Jena
Loebdergraben 32, 07740 Jena, Germany
Telephone: *49-3641-948813
Fax: *49-3641-948812
Ralf.Hesse@uni-jena.de

## ABSTRACT

The SRTM data set is the highest resolution DEM with global or continental coverage. It is therefore the DEM of choice for continental-scale geomorphological mapping and quantitative analysis. In this study, SRTM data are used for the identification and characterisation of endorheic basins in southern South America (south of 19°S). The results show the feasibility of continental-scale quantitative geomorphology based on SRTM data and provide insights into the distribution of closed basins. The largest endorheic basin is located in the Puna region and consists of several interconnected sub-basins. This basin accounts for 38.6 % (7877 $km^3$) of the total volume of the endorheic basins identified in this study. Analyses of the geographic distribution show a narrow longitudinal distribution between 64.5 and 71.5° W and a multimodal latitudinal distribution which is characterised by two groups of basins at 22.5–27.5°S and 37.5–50.0° S and an almost complete absence of basins between 27.5 and 37.5° S. Problems and sources of misinterpretation arising from data quality and resolution are discussed. Further research, targeting in particular the genesis and potential for paleoenvironmental reconstruction of closed basins in southern Argentina, is called for.

**Keywords: SRTM, quantitative geomorphology, endorheic basins, South America**

## 1. INTRODUCTION

Endorheic basins are characteristic geomorphic features in southern South America. Their geographic distribution reflects the long-term persistence of semiarid to arid conditions which prevent both breaching and rapid infilling of these depressions. Several endorheic basins in South America have been investigated, in particular with the aim to reconstruct paleoenvironmental conditions and changes. The most notable include the Andean basins of the Salar de Atacama (e.g. Bobst et al., 2001; Lowenstein et al., 2003), the Salar de Uyuni (Baker et al., 2001) and several basins in the Puna region (Strecker et al., 2007, and references therein). Several extra-Andean endorheic basins of Argentina have been studied (e.g. Alonso, 2006; Schäbitz, 1999), in particular Lago Cardiel (e.g. Galloway et al., 1988; Markgraf et al., 2003; Beres et al., 2008).

The aim of this paper is to demonstrate the use of SRTM data for continental-scale quantitative geomorphology and to draw attention to the geographic distribution of endorheic basins in South America south of 19°S. In particular, the methodology and results of a quantitative mapping of endorheic basins based on SRTM data are presented.

## 2. DATA AND METHODS

The approach presented here is based on 3 arc second resolution SRTM version 2 data of South America south of 19°S (NASA, 2006). The SRTM tiles were mosaicked and missing data values were filled in by interpolation. To identify endorheic basins, topographic depressions in the DEM were filled using the algorithm after Planchon and Darboux (2001) with enforced drainage on flats which is implemented in the TAS (Terrain Analysis System) software version 2.0.9 by John Lindsay (Lindsay, 2005). Due to the large amount of data, this was done in segments of 10000 by 6000 pixels. Subsequently, the original DEM was subtracted from the depression-filled DEM. The difference DEM holds pixel-specific depths of closed basins.

The individual pixels were combined using a three-step merging algorithm which was implemented in VBA under MS Excel. All pixels with depth values larger than zero were considered basin pixels (i.e. to represent parts of closed basins). Pixels were combined in the same object (basin) if they were immediate vertical of horizontal neighbours. As the DEM was processed line by line from north to south in the first step, new object numbers were assigned to every basin pixel with no basin pixel to its left (west); basin pixels bordered by a basin pixel to the left were assigned the object number of this pixel. A list of latitudinally connected objects was created based on neighbourhood relationships with the previous DEM line. In a second step, this list was used to group and assign identical object numbers to connected objects. In a third step, circular links were resolved by an iterative search for linked objects which had not been assigned corresponding object numbers in the second step. As a result, all linked basin pixels carry the same object number unique to the respective basin.

For all objects, the following parameters were extracted from the closed basin depth DEM: basin area, mean and maximum depth, volume and centre coordinates. The calculation of basin area and volume is based on rectangular pixel areas calculated from pixel latitudes assuming a spherical Earth with a radius of 6367.445 km (mean of the WGS-84 ellipsoid half axes; NIMA, 2000). Mean basin depth was calculated as the mean depth weighted by area. Basin centre coordinates were calculated as mean centre coordinates weighted by basin volume.

The identification of closed basins was validated by locating all objects with volumes ≥ 2 km$^3$ in high-resolution satellite images (DigitalGlobe, 2007). In many cases this also allowed assigning names to basins, lakes or salars. Only confirmed endorheic basins were included in the following analyses. Size-frequency distributions as well as spatial distributions were calculated.

## 3. RESULTS

### 3.1 VALIDATION, OVERVIEW AND EXAMPLES

The total number of unique objects identified using the described approach is 9234323. However, it has to be noted that most of the basins have sizes of only a few pixels and depths of ≤ 5 m. Many of them likely have to be considered artefacts attributable to the properties of the SRTM data (cf. section 4.1.). Therefore, only objects with volumes ≥ 2 km$^3$ are considered. These account for 96.5 % of the total basin volume before validation.

Of the 289 objects ≥ 2 km$^3$, 251 were validated to be endorheic basins. However, because all 38 erroneously identified basins are small (<25 km$^3$), they account for only 1.1% of the total volume (Table 1). In the following analyses, only validated endorheic basins are used.

The total volume of the 251 confirmed endorheic basins in South America south of 19°S with volumes ≥2 km$^3$ was found to be 20404 km$^3$. The largest endorheic basin is located in the Puna region and consists of the interconnected sub-basins of Salar de Arizaro, Salar de Antofalla, Salar Pocitos, Salina de Rincón, Salar del Hombre Muerto and Salar de Cauchari. With a volume of 7877 km$^3$, this accounts for 38.6 % of the total volume of endorheic basins. It covers an area of 23009 km$^2$ (12.3% of the total area) and has a maximum depth of 801 m and a mean depth of 342 m.

The size-frequency distribution of endorheic basins (Figure 1) is characterised by a very small number of very large basins and a large number of small basins and can be described by the power function $V = 8705\ N^{-1.5026}$ with V = basin volume and N = number of basins. The ten largest basins (by volume) together account for 78.4% of the total volume and for 40.8% of the total area. Table 2 gives an overview of the largest 25 endorheic basins which together account for 87.7 % of the total volume and 66.4 % of the total area or endorheic basins ≥ 2 $km^3$.

**Table 1** – Validation results.

| Basin volume [$km^3$] | Erroneously identified basins | Validated basins |
|---|---|---|
| > 4096 | 0 | 1 |
| 2048 – 4096 | 0 | 2 |
| 1024 – 2048 | 0 | 0 |
| 512 – 1024 | 0 | 1 |
| 256 – 512 | 0 | 5 |
| 128 – 256 | 0 | 8 |
| 64 – 128 | 0 | 13 |
| 32 – 64 | 0 | 12 |
| 16 – 32 | 3 | 26 |
| 8 – 16 | 5 | 38 |
| 4 – 8 | 11 | 56 |
| 2 – 4 | 19 | 89 |
| Total | 38 | 251 |

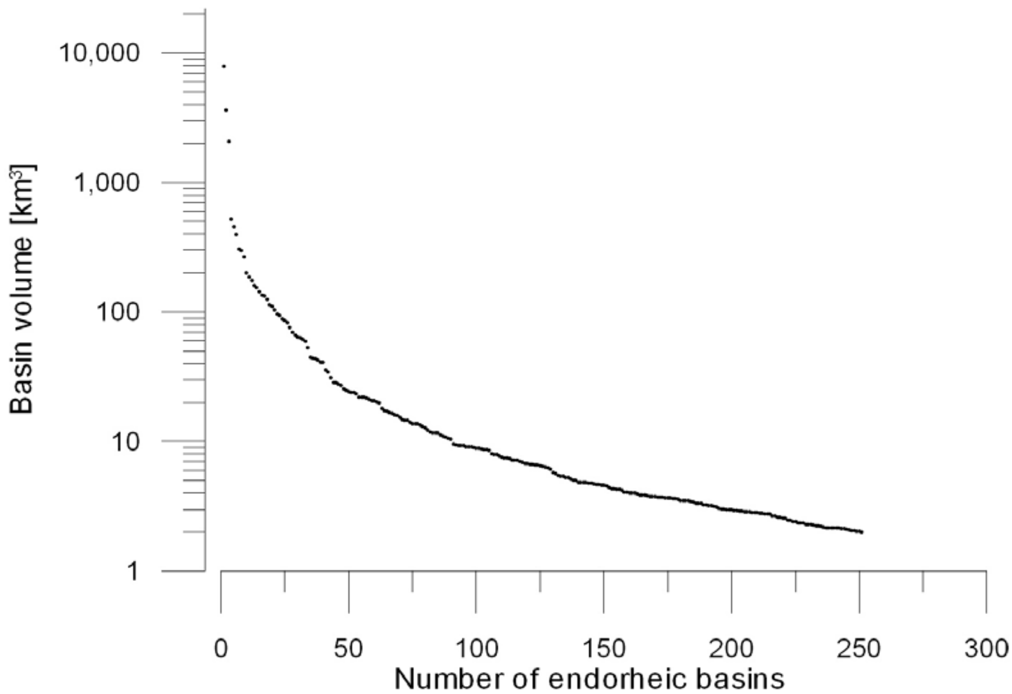


**Figure 1 –** Size-frequency distribution of endorheic basins.

**Table 2** – Properties of the largest 25 endorheic basins (sorted by basin volume).

| Volume [km³] | Area [km²] | Depth [m] | | Centre latitude | Centre longitude | Place names |
|---|---|---|---|---|---|---|
| | | max. | mean | | | |
| 7877.4 | 23008.8 | 801 | 342 | 24.95 | 67,45 | Puna de Argentina with Salar de Arizaro, Salar de Antofalla, Salar Pocitos, Salina de Rincón, Salar del Hombre Muerto, Salar de Cauchari |
| 3613.1 | 8513.9 | 616 | 424 | 23.35 | 67,99 | Salar de Atacama |
| 2067.8 | 4619.0 | 923 | 448 | 26.37 | 67,47 | basin of Laguna Carachi Pampa and Laguna de Antofagasta |
| 519.2 | 3972.8 | 266 | 131 | 38.11 | 68,90 | Cuenca del Añelo |
| 453.6 | 5287.5 | 158 | 86 | 23.41 | 65,94 | Salar de Guayatayo, Salinas Grandes |
| 395.4 | 3779.4 | 211 | 105 | 40.38 | 65,31 | Gran Bajo del Gualicho |
| 305.4 | 5469.6 | 104 | 56 | 42.96 | 66,85 | Bajo de la Tierra Colorado |
| 298.1 | 2464.3 | 327 | 121 | 48.02 | 70,44 | |
| 265.1 | 936.3 | 527 | 283 | 25.16 | 68,13 | Salar de Rio Grande |
| 200.4 | 18327.9 | 72 | 11 | 20.37 | 67,84 | Salar de Uyuni, Salar de Coipasa, Salar de Laguani |
| 187.0 | 692.8 | 612 | 270 | 25.57 | 68,38 | |
| 174.5 | 2959.5 | 141 | 59 | 39.74 | 66,92 | Bajo de los Menucos (central basin) |
| 159.4 | 749.7 | 384 | 213 | 25.76 | 68,60 | Salar de La Isla, Salar de Las Pariñas |
| 153.7 | 617.9 | 452 | 249 | 24.81 | 68,30 | |
| 143.6 | 9497.9 | 44 | 15 | 29.93 | 65,17 | Salinas Grandes |
| 134.8 | 2907.4 | 114 | 46 | 40.49 | 66,16 | Bajo de los Menucos (eastern basin) |
| 132.8 | 3208.8 | 116 | 41 | 41.20 | 69,31 | Bajo de Cari Laufquen |
| 125.4 | 19065.9 | 20 | 7 | 30.93 | 63,25 | Laguna Mar Chiquita |
| 113.5 | 1012.7 | 280 | 112 | 23.72 | 68,97 | Salar Los Morros, Salar Santa Elvira |
| 110.6 | 1610.0 | 156 | 69 | 42.54 | 68,24 | Pampa de Gan Gan |
| 104.0 | 957.6 | 140 | 109 | 48.88 | 71,17 | Lago Cardiel |
| 96.1 | 338.7 | 525 | 284 | 25.83 | 68,91 | Salina de Aguliar |
| 94.0 | 305.7 | 572 | 308 | 24.27 | 67,94 | |
| 88.6 | 1248.6 | 153 | 71 | 43.78 | 69,72 | Pampa de Agnia |
| 85.8 | 2569.3 | 102 | 33 | 47.82 | 67,96 | Lago Grande |

## 3.2. SPATIAL DISTRIBUTION OF ENDORHEIC BASINS

The geographic distribution of endorheic basins (Figures 2 and 3) is characterised by a narrow longitudinal distribution and multimodal latitudinal distribution. In terms of the longitudinal distribution, most (98.2 % of the volume) of the validated endorheic basins are located between 64.5 and 71.5° W. 85.2 % lie within an even narrower range between 66.5 and 69.0° W. The multimodal latitudinal distribution consists of two disjoint groups of basins. The northern group between 22.5 and 27.5°S represents the Andean basins and accounts for 78.0 % of the volume of all basins. The southern group between 37.5 and 50.0°S (located mainly in Patagonia) accounts for 17.3 % of the volume of all basins. The two groups are separated by an almost complete lack of endorheic basins between 27.5 and 37.5° S. Together the two groups represent 95.3 % of the volume of all endorheic basins, i.e. only 4.7 % of the total basin volume is located in the combined latitudinal segments 19.0–22.5° S, 27.5–37.5° S and 50.0–56.0° S.

The map of the geographic distribution (Figure 4 a) shows that some spatially extensive basins are present between the two groups. However, these basins are relatively shallow and therefore have only low volumes. Differences in distribution and morphology between the two groups of basins can be discerned in Figures 4 b and 4 c. The basins in the northern region are closely spaced. The alignment of many of these basins along mountain ranges indicates a genetic relation to Andean orogeny. In contrast to this, the basins of the southern region are not aligned along mountain ranges. They occur both in lowland regions which are characterised predominantly by fluvial geomorphology and in extra-Andean highlands which are characterised by Cenozoic volcanism (cf. D'Orazio et al., 2004).

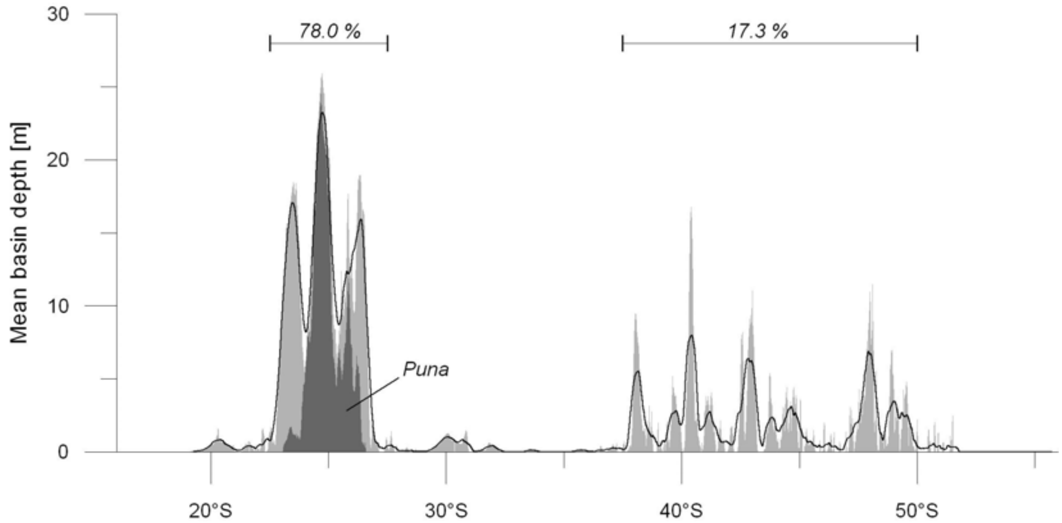


**Figure 2 –** Longitudinal distribution (mean basin depth as basin volume divided by land area) of endorheic basins (light grey, black line: 0.5° running average). Puna basins shown in dark grey.

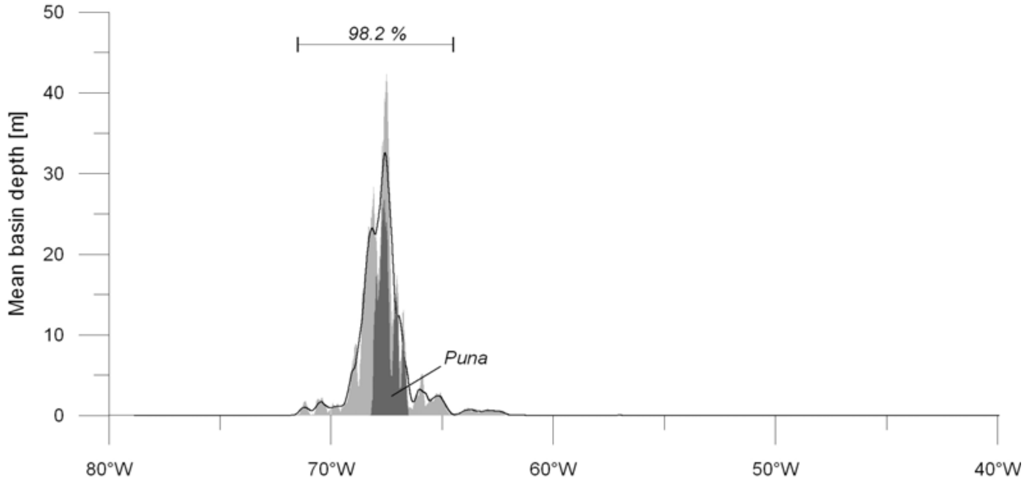


**Figure 3** – Latitudinal distribution (mean basin depth as basin volume divided by land area) of endorheic basins (light grey, black line: 0.5° running average). Puna basins shown in dark grey.

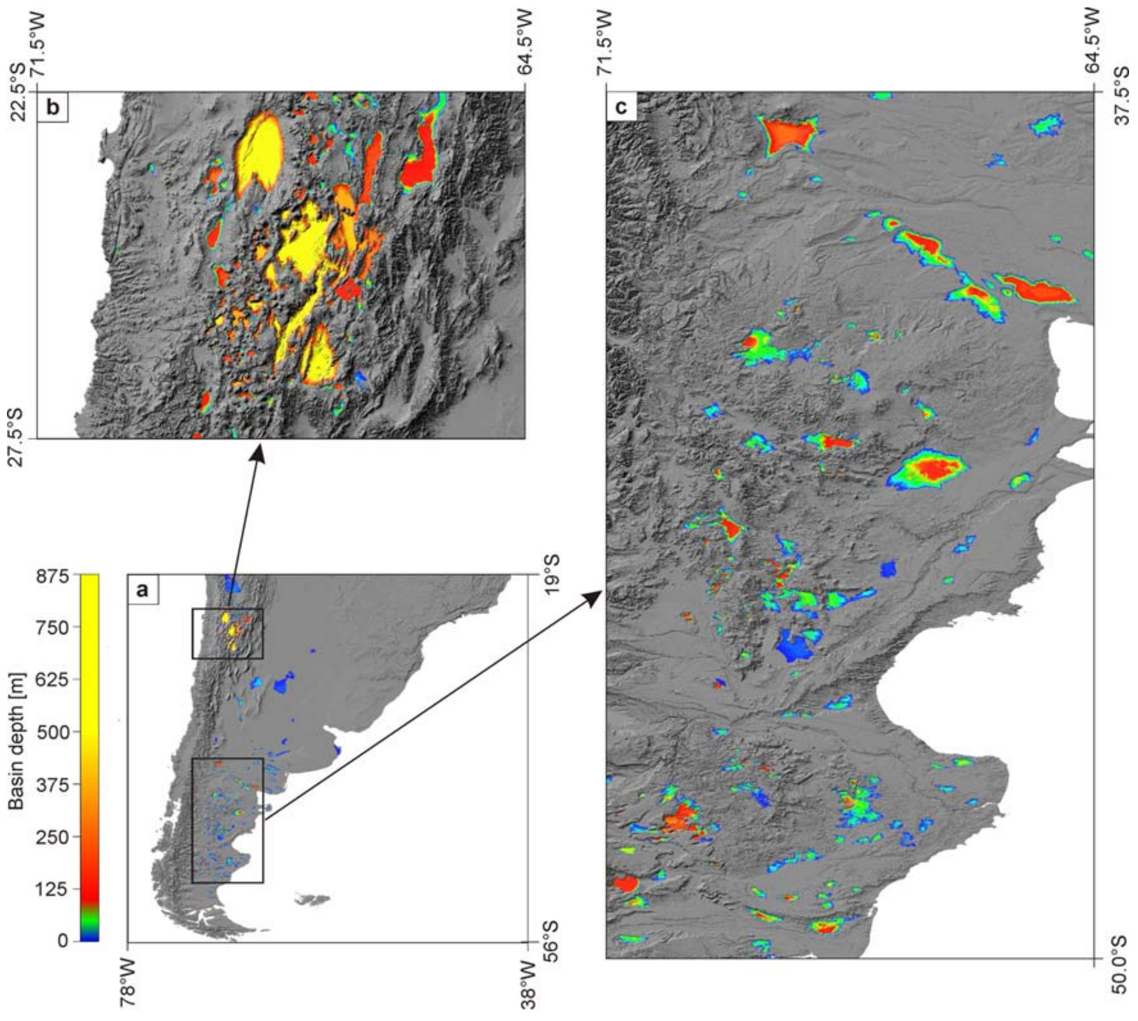


**Figure 4** – Distribution of endorheic basins in southern South America. **a** – overview; **b** – northern group of basins; **c** –southern group of basins.

## 4. DISCUSSION AND CONCLUSIONS

### 4.1. VALIDATION AND DATA QUALITY ISSUES

The results presented here show the feasibility of continental-scale use of SRTM data for the delineation and quantitative characterisation of endorheic basins. Quantitative parameters of geomorphic features (e.g. depth, area, volume, spatial distribution and size-frequency relationships of endorheic basins) can be extracted using suitable algorithms. However, there are reasons for cautionary remarks regarding potentially erroneous identification of individual features. While 251 of the largest 289 features identified in this study were validated as closed basins, 38 features (accounting for 1.1 % of the total volume) were erroneously identified. This can be attributed to three sources of error: (i) Data scatter, e.g. due to vegetation, may result in numerous spurious pits in the SRTM DEM. A high density of interconnected pits may lead to the erroneous identification of spatially extensive shallow basins. (ii) In areas of high relief, the spatial resolution of the SRTM data may be too coarse to properly delineate narrow drainage, thus resulting in apparent basins upstream of very narrow valley segments. (iii) Seemingly closed basins may also result from the interpolation of missing values in the DEM. Again, this issue is particularly important in areas of steep relief where radar shadow has caused missing data. For these reasons, validation of individual basins (in this study by visual geomorphological analysis of high-resolution satellite images) is necessary. Besides the erroneous identification of closed basins, the three sources of error may also lead to inaccuracies in the depth (and concomitantly in the area and volume) of identified basins and may therefore be reasons for quantitative and geomorphologic misinterpretations. As all three identified sources of error lead to an overestimation of basin depths, the depths, areas and volumes of endorheic basins in this study are maximum values.

### 4.2. INTERPRETATION AND RESEARCH POTENTIAL

The distribution of endorheic basins within a narrow longitudinal range which is characterised by arid to semi-arid climate indicates that their preservation is linked to the long-term persistence of generally arid conditions. The existence of a marked gap in the distribution of endorheic basins can not be attributed to the breaching or infilling of previously existing basins as this gap is situated in the latitudinal centre of an extensive arid belt and climatic changes are generally considered to involve latitudinal displacements of climate zones (e.g. Messerli et al., 1993). Rather, the differences in the distribution of endorheic basins likely has to be attributed to differences in their genesis.

However, questions regarding the genesis and geological history of the disjoint groups of endorheic basins are only partially resolved. The largest basin, the Puna with Salar de Arizaro, Salar de Antofalla, Salar Pocitos, Salina de Rincón and Salar del Hombre Muerto and Salar de Cauchari has been shown to be of tectonic origin (Voss, 2002). It contains approximately 900 m of evaporites (Vinante and Alonso, 2006), recording long-term persistence of internal drainage and generally arid conditions for at least 14.1 Ma (Alonso et al., 1991; Vandervoort et al., 1995). The Salar de Atacama basin – the second largest endorheic basin identified in this study – is also of tectonic origin (Reutter et al., 2006) with internal drainage possibly since the Oligocene (Horton et al., 2002), tectonic fault activity continuing into the late Quaternary and a quasi-continuous evaporitic stratigraphy over the last 325 ka (Lowenstein et al., 2003). For most extra-Andean endorheic basins, age and formative processes are unknown. In many cases, large-scale geomorphology lets a tectonic genesis appear likely. Some basins may be of volcanic (caldera) origin (cf. Aragón et al., 1996). Most of the shallow, elongate basins of the Argentinean Pampa region which are likely attributable to aeolian deflation are smaller than 2 $km^3$ and hence not considered in the present study. Other small basins, e.g. Bajo Hondo, have been interpreted as possible impact craters (Rocca, 2005).

Endorheic basins in southern South America record tectonic and paleoenvironmental changes at least since the Miocene. Evaporitic, lacustrine and fluvial sediments have been documented in many basins, and high resolution satellite images (DigitalGlobe, 2007) allow the identification of paleo-shorelines in numerous basins. Given the large number, geomorphic properties and geographic distribution of endorheic basins in southern South America, their full potential for research – in particular regarding their genesis and paleoenvironmental changes – is far from being realised.

**ACKNOWLEDGEMENTS**

I wish to thank Gerhard Daut who sparked my interest in the endorheic basins of South America and Antje Ober who helped developing the merging algorithm.

## 5. REFERENCES

Alonso, R.N. 2006. Ambientes evaporíticos continentales de Argentina. INSUGEO, Serie Correlación Geológica, v. 21, p. 155-170.

Alonso, R.N., Jordan, T.E., Tabbutt, K.T., Vandervoort, D.S. 1991. Giant evaporite belts of the Neogene central Andes. Geology, v. 19, n. 4, p. 401-404.

Aragón, E., Rodriguez, A.M.I, Benialgo, A. 1996. A calderas field at the Marifil Formation, new olcanogenic interpretation, Norpatagonian Massif, Argentina. Journal of South American Earth Sciences, v. 9, n. 5/6, p. 321-328.

Baker, P.A., Rigsby, C.A., Seltzer, G.O., Fritz, S.C., Lowenstein, T.K., Bacher, N.P., Veliz, C. 2001. Tropical climate changes at millenial and orbital timescales on the Bolivian Altiplano. Nature, v. 409, p. 698-701.

Beres, M., Gilli, A., Ariztegui, D., Anselmetti, F.S. 2008. The Lago Cardiel Basin, Argentina (49°S): Origin and evolution revealed by high-resolution multichannel seismic reflection studies. Journal of South American Earth Sciences, v. 25, n. 1, p. 74-85.

Bobst, A.L., Lowenstein, T.K., Jordan, T.E., Godfrey, L.V., Ku, T.-L., Luo, S. 2001. A 106 ka paleoclimate record from drill core of the Salar de Atacama, northern Chile. Palaeogeography, Palaeoclimatology, Palaeoecology, v. 173, p. 21-42.

DigitalGlobe. 2007. Landsat and Quickbird images. Access through Google Earth.

D'Orazio, M., Innocenti, F., Manetti, P., Haller, M.J. 2004. Cenozoic back-arc magmatism of the southern extra-Andean Patagonia (44° 30' - 52° S): A review of geochemical data and geodynamic interpretation. Revista de la Asociación Geológica Argentina, v. 59, n. 4, p. 525-538.

Galloway, R.W., Markgraf, V., Bradbury, J.P. 1988. Dating shorelines of lakes in Patagonia, Argentina. Journal of South American Earth Sciences, v. 1, n. 2, p. 195-198.

Horton, B.K., Hampton, B.A., Lareau, B.N., Baldellón, E. 2002. Tertiary Provenance History of the Northern and Central Altiplano (Central Andes, Bolivia): A Detrital Record of Plateau-Margin Tectonics. Journal of Sedimentary Research, v. 72, n. 5, p. 711-726.

Lindsay, J. 2005. The Terrain Analysis System: a tool for hydro-geomorphic applications. Hydrological Processes, v. 19, p. 1123-1130.

Lowenstein, T.K., Hein, M.C., Bobst, A.L., Jordan, T.E., Ku, T.-L., Luo, S. 2003. An Assessment of Stratigraphic Completeness in Climate-Sensitive Closed-Basin Lake Sediments: Salar de Atacama, Chile. Journal of Sedimentary Research, v. 73, n. 1, p. 91-104.

Markgraf, V., Bradbury, J.P., Schwalb, A., Burns, S.J., Stern, C., Ariztegui, D., Gilli, A., Anselmetti, F.S., Stine, S., Maidana, N. 2003. Holocene palaeoclimates of southern Patagonia: limnological and environmental history of Lago Cardiel, Argentina. The Holocene, v. 13, n. 4, p. 581-591.

Messerli, B., Grosjean, M., Graf, K., Shotterer, U., Schreier, H., Vuille, M. 1993. Climate change and natural resource dynamics of the Atacama Altiplano during the last 18 000 years: a preliminary synthesis. Mountain Research and Development, v. 13, n. 2, p. 117-127.

NASA. 2006. SRTM version 2, ftp://e0srp01u.ecs.nasa.gov/srtm/version2 (download: 13.07.2006).